SolarPACES 2024, 30th International Conference on Concentrating Solar Power, Thermal, and Chemical Energy Systems

CSP Integration, Markets, and Policy

https://doi.org/10.52825/solarpaces.v3i.2515

© Authors. This work is licensed under a Creative Commons Attribution 4.0 International License

Published: 09 Oct. 2025

# Demonstration of a Proof-of-Concept Integrated Skip Hoist-Thermal Energy Storage System

Nader S. Saleh<sup>1,2</sup>, Shaker Alaqel<sup>3</sup>, Eldwin Djajadiwinata<sup>1,2</sup>, Rageh Saeed<sup>1,2</sup>, Hany Al-Ansary<sup>1,2</sup>, Zeyad Al-Suhaibani<sup>1</sup>, Abdelrahman El-Leathy<sup>1,2,4</sup>, Syed Danish<sup>5</sup>, and Sheldon Jeter<sup>6</sup>

<sup>1</sup>Mechanical Engineering Department, King Saud University, Saudi Arabia
<sup>2</sup>K.A.CARE Energy Research and Innovation Center at Riyadh, Saudi Arabia
<sup>3</sup>Sandia National Laboratories, Mechanical Engineering, PhD, USA
<sup>4</sup>Mechanical Power Engineering Dept., Helwan University, Egypt
<sup>5</sup>Sustainable Energy Technologies Center, King Saud University, Saudi Arabia
<sup>6</sup>Georgia Institute of Technology, School of Mechanical Engineering, USA
\*Correspondence: Nader S. Saleh, nader.alhabtary@outlook.com

**Abstract.** This paper presents the design, construction, and preliminary testing of an innovative skip-hoist particle lift (PL) integrated with a multi-layered cylindrical thermal energy storage (TES) system for particle-based concentrated solar power (CSP) applications. The skip-hoist PL, constructed with stainless steel for high-temperature compatibility, was seamlessly integrated with two TES bins on a 22-m concrete tower. Preliminary testing at ambient temperature confirmed the system's operational feasibility, paving the way for high-temperature testing and the proposed 1.3 MWe pre-commercial scale-up in Waad Al-Shamal, Saudi Arabia.

Keywords: Thermal Energy Storage, Skip-Hoist Particle Lift, Concentrated Solar Power

## 1. Introduction

CSP is a promising renewable energy technology that captures sunlight to generate electricity. In recent years, there has been increasing interest in utilizing small solid particles, such as sand, as both heat capture and energy storage medium within CSP systems, owing to their unique properties and inherent advantages, such as lack of freezing issues and corrosivity, low cost, abundant availability, low agglomeration tendency, high heat capacity, and high temperature limit [1]. Since 2009, collaborative research initiatives between King Saud University (KSU) and the Georgia Institute of Technology (GIT) have extensively explored the non-commercialized components of particle-based CSP technology. By 2016, a proof-of concept CSP system was developed at Riyadh Valley Company (RVC) on the KSU campus, comprising a particle heating receiver (PHR) atop a tower, a thermal energy storage (TES) bin, a particle lift (PL), and a heliostat field. In late 2016, a collaboration between KSU and the Saudi Electricity Company (SEC) facilitated the installation of the remaining components, leading to the establishment of the world's first proof-of-concept particle-based CSP plant, with a peak thermal power output of approximately 300 kW [2]. This successful proof-of-concept phase has prompted KSU and SEC to consider the next phase: developing a 1.3 MW<sub>e</sub> pre-commercial scale-up of the system to evaluate its economic viability. The proposed site for this demonstration project is located in Waad Al-Shamal (31.66°N, 38.86°E), Saudi Arabia [3]. To advance

this initiative, two enabling technologies are to be tested at a suitable scale: (1) an efficient, reliable, cost-effective, and high-temperature particle lift, and (2) a low-cost, well-insulated thermal energy storage system. Existing particle lifting mechanisms commonly utilized in construction and mining, such as screw-type or Olds elevators, bucket elevators, conveyor belts, and skip-hoist lifts, exhibit several limitations, including low mechanical efficiency, temperature constraints, scalability challenges, cost implications, integration complexities, excessive particle attrition, and large area for heat loss. The KSU particle-based CSP plant employed an Olds elevator, which encountered most of these challenges. Consequently, the selection of an appropriate particle lift for seamless integration into the particle-based CSP system has been a key area of research for the collaborative research team from KSU and GIT. Through rigorous evaluation, the skip-hoist lift emerged as the most suitable design option to address both current and future requirements for small and large-scale commercial particle-based CSP plants while ensuring high thermal and mechanical efficiency [4]. In terms of the TES system, KSU's design philosophy focuses on simplicity and cost efficiency, leading to the development of a cylindrical, multi-layered structure that has been tested in prior evaluations [5]. This design incorporated four layers, arranged from innermost to outermost: (1) alumina-rich insulating firebrick (IFB), (2) perlite concrete with refractory cement, (3) expansion joint board, and (4) reinforced concrete. However, this configuration presents two notable concerns: the inherent brittleness of the IFB and the shrinkage tendency of perlite aggregates. Over time, continual particle flow against the IFB layer can lead to erosion, adversely affecting the thermal performance of the TES system and causing particle contamination. The IFB and perlite concrete layers serve as thermal barriers; thus, alternative materials must be identified to replace these components. Following a comprehensive material survey, calcium silicate was determined to be the most suitable candidate for substituting the IFB and perlite layers. To protect the calcium silicate layer from particle abrasion, an additional layer with high abrasion resistance is necessary to be placed between the particles and the calcium silicate layer. A prototype system incorporating the new designs for the PL and TES subsystems has been constructed on the KSU campus. This manuscript provides a detailed description of this innovative system.

# 2. Skip-hoist particle lift

The skip-hoist particle lift (PL) comprises several interconnected components, including a preskip, a skip, an upper hopper, an electric winch/winder, and guide rails. The pre-skip is responsible for filling the skip with particles, which are then transported to the upper hopper. The skip moves between the pre-skip and the upper hopper along the guide rails, with the winder facilitating this movement. A wooden model of the PL was constructed to demonstrate the functionality and interaction of these components. Following successful testing of this model, a design for a high-temperature system was developed. Stainless steel (SS316) was chosen for the components that come into contact with high-temperature particles, while mild steel was selected for the remaining parts. Figure 1 shows both the wooden model and the high-temperature design.

The pre-skip, Figure 2a, was designed to accommodate particles that can fully fill the skip's volume. It features a pivoting chute and a sliding door, with thermal insulation applied externally. The operation of the pivoting chute is activated by the arrival and departure of the skip. The skip, Figure 2b, is designed to travel a vertical distance of around 35 meters, carrying approximately 120 kg of particles at a nominal speed of 2 m/s. Its inner liner has a square cross-section (0.28 m²) and a height three times its width, effectively minimizing the ullage volume caused by the angle of repose, resulting in a total volume of about 0.07 m³. The inner liner is constructed from stainless steel (SS316), while the outer cladding is made of mild steel. The space between the inner and outer liners is filled with thermal insulation, and the skip is equipped with a thermally insulated lid. The upper hopper, depicted in Figure 2c, is designed to hold a particle volume of 0.12 m³. Its design incorporates several features, such as a double air-blocking door to minimize air entrainment and infiltration, thereby reducing advective heat

loss. Additionally, a silicon carbide (SiC) foam filter is included to prevent particle contamination.

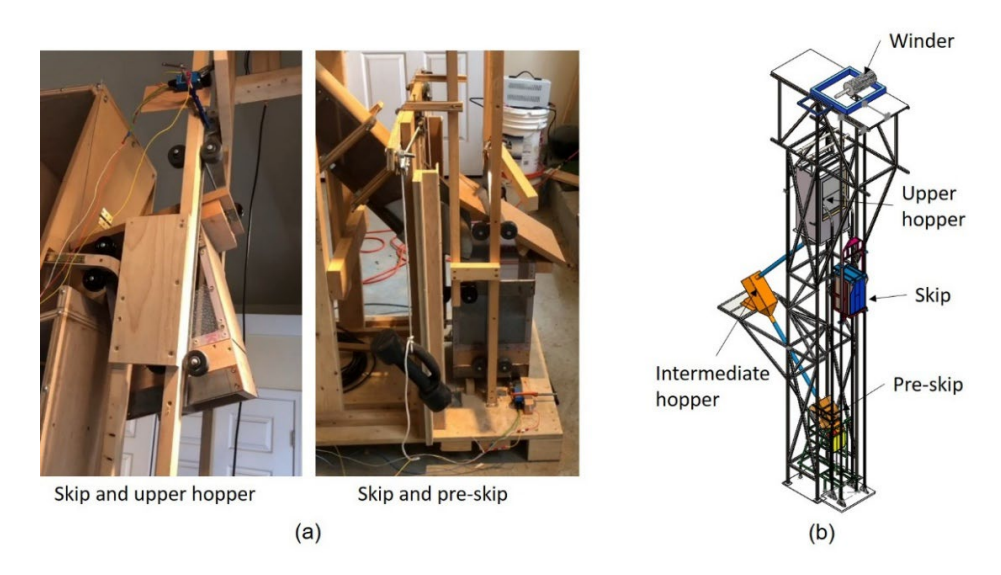


Figure 1. (a) Wooden PL model, (b) high-temperature PL design

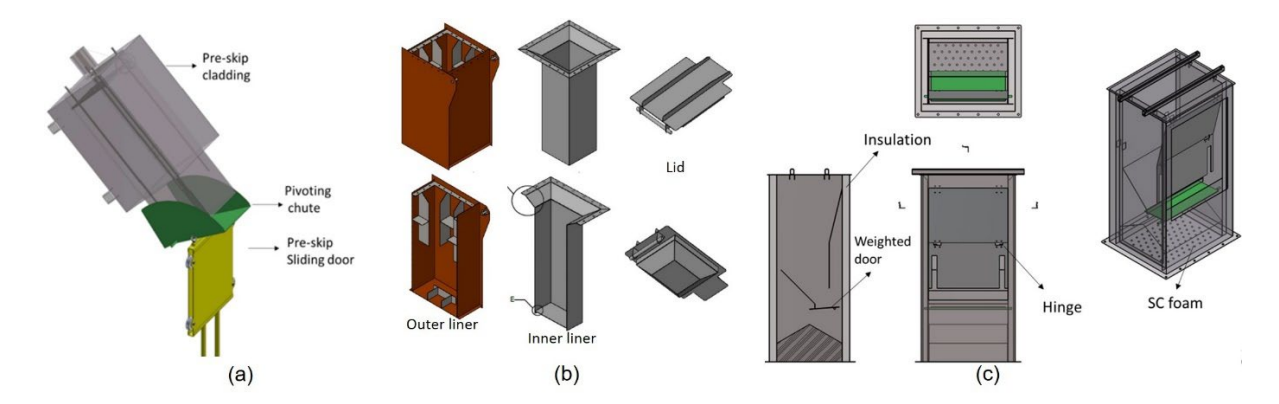


Figure 2. (a) Pre-skip, (b) skip, (c) upper hopper

The guide rails are designed to continuously engage the guide rollers on the skip body with one rail, while another rail interacts with the guide rollers on the lifting bail throughout the entire travel distance. The electric winch/winder is tasked with raising the skip to the level of the upper hopper and lowering it back to the pre-skip level. The technical specifications of the winch are detailed in Table 1. The electric winch is equipped with an automatic control system. The control system is composed of a variable frequency drive (VFD, model: EV510A:2), a programmable logic controller (PLC, model: SIMATIC S7-200), a height encoder (OMRON E6B2-CWZ5B), limit switches, and several relays. The PLC is provided with a touch screen where the desired/required inputs are entered.

Table 1. Specifications of the JK5 winch

Parameter	Value
Maximum pulling force (kg)	500
Lifting speed (m/s)	variable speed, maximum: 2
Steel wire rope (diameter: mm, length: m)	14, 50
Drum size (diameter: mm, length: mm)	377, 750

Figure 3 shows the components of the PL system during the fabrication stage and after being installed and integrated. This integration is a critical step in ensuring the smooth operation of the particle lift system. Prior to the start of automatic operation, the height encoder must be calibrated. The number of pulses per meter, for the skip to rise or fall, must be determined and entered to the PLC through the touch screen. The height encoder is connected to the shaft of the winch's drum using a coupling and an angle bracket. The encoder communicates with the PLC, which in turn communicates with the VFD based on the signal provided by the encoder, so that the speed and direction of the winch's motor are controlled. To determine the optimal speed, elevation for each stage, and the dwell time needed at the pre-skip and upper hopper levels, a thorough investigation was conducted.



Figure 3. Skip-hoist PL during fabrication and after installation

The skip's journey is divided into three stages as can be seen in Figure 4. The skip starts its journey at Level 0, where it communicates with the pre-skip. The skip requires a brief dwell time (less than 5 s) to be filled with particles. Once the charging process is complete, the skip is pulled upward with low speed (0.1 m/s), enabling a smooth closure of the pre-skip's pivoting chute. Upon reaching Level 1, the skip is then accelerated, reaching its maximum speed (2 m/s). As the skip approaches the upper hopper (Level 2), it begins to decelerate (0.1 m/s). Upon reaching Level 3, a dwell time is required to ensure the complete delivery of the skip's load to the upper hopper. The return journey of the skip follows the same protocol as the departure.

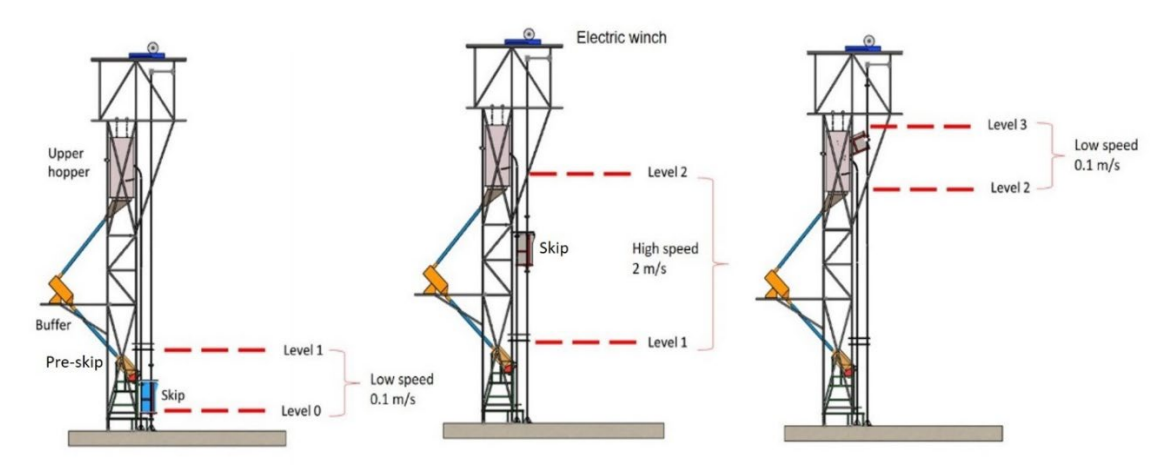


Figure 4. PL's operation, stages of the skip's journey during rise and fall

In this experiment, the skip has two speeds connected by brief acceleration or deceleration. In this case, the high speed is limited by the speed of the available winder (2.0 m/s), Table 1. In other cases, the ultimate speed will be limited by the allowable speed of the hoisting rope, which can be much higher. In the finalized design, the acceleration and maximum speed of the skip will be determined from an overall design and optimization study. Obviously, a high maximum speed has the advantage of yielding a smaller and more economical skip at the cost of a more expensive winder and related components. The low speed or creep speed is selected to allow safe docking of the skip. Since the skip-hoist PL will usually be in a funicular or double skip arrangement, the trajectory must be symmetrical so that the low creep speed must be the same at top and bottom. Based on industrial practice this speed should be a small fraction of the full speed; so, a safely low speed of 0.1 m/s was selected for this preliminary application. The current experiment was built to demonstrate feasibility and to reveal any unexpected operational issues. After this experiment, the design will be optimized for costs, heat loss, and parasitic power consumption.

## 3. TES system

The design and selection of materials for thermal energy storage (TES) bins are critical in determining the cost competitiveness of electricity relative to other renewable energy technologies. Furthermore, the TES system experiences significant thermal cycling, which induces considerable thermal and structural stresses, increasing its susceptibility to fracture. Therefore, it is essential to utilize materials with excellent insulation properties and a low coefficient of thermal expansion. A well-insulated TES system can maintain particles at elevated temperatures for extended periods, thereby enhancing the plant's availability and minimizing downtime. The proposed design of the TES bin addresses several challenges including minimized heat loss at high temperature, ensuring low cost with massive containment, maintaining structural integrity, and facilitating construction.

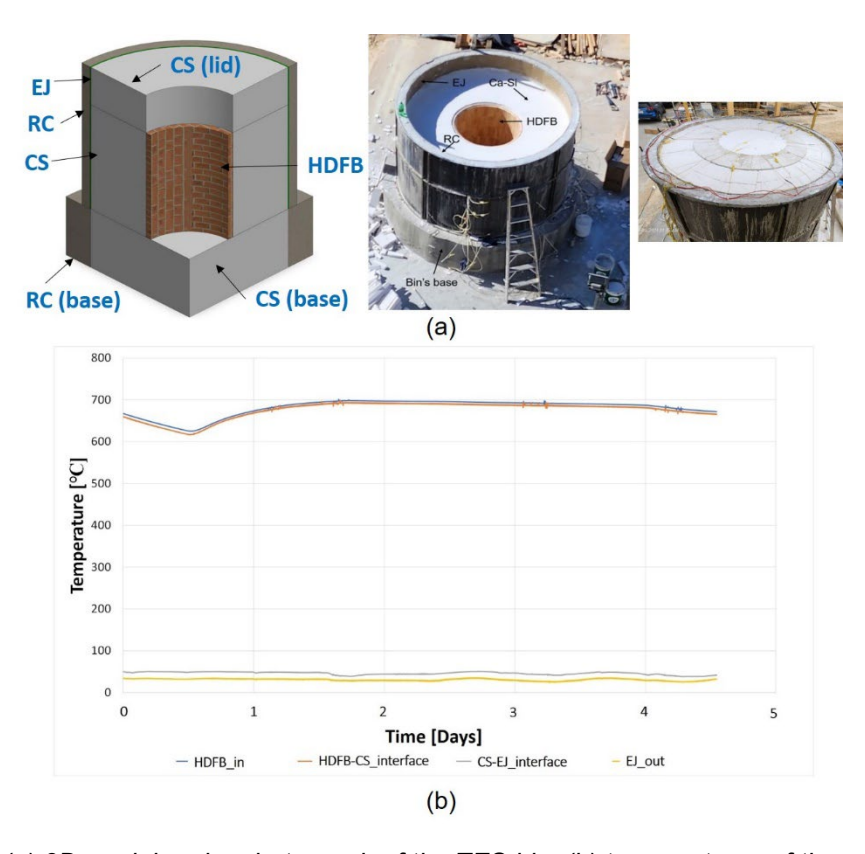


Figure 5. (a) 3D model and a photograph of the TES bin, (b) temperatures of the wall layers

The TES bin features a cylindrical multi-layered wall composed of four layers arranged from innermost to outermost: (1) high-density firebrick (HDFB), (2) calcium silicate (CS), (3) expansion joint (EJ), and (4) reinforced concrete (RC). The HDFB layer protects the CS layer from abrasion caused by particle flow, while the CS layer provides required thermal insulation and fire resistance. The EJ layer allows for flexibility, accommodating any expansion or contraction of the inner layers due to temperature variations. The RC layer provides structural strength and durability, protecting the inner layers from harsh external conditions. The HDFB layer is constructed from Mullite firebricks (75% alumina), specifically designed to prevent inward collapse, eliminate the need for mortar, and simplify assembly. The CS layer is made from calcium silicate boards, and the EJ layer consists of recycled bitumen fiber boards, which exhibit high compression and recovery rates (95%) and a compressive strength of ≥ 2 MPa. A small-scale TES bin, with a volume of approximately 1 m<sup>3</sup>, has been constructed to demonstrate the feasibility of this design, as shown in Figure 5a. The bin was filled with white sand, which was electrically heated to 700 °C. Throughout the experiment, the temperatures of the wall layers and the heat flux through the wall were continuously monitored. Additionally, the thickness of the expansion joint (EJ) layer was measured at three key points: before the test commenced, when the sand reached 700 °C, and after the bin cooled down to atmospheric temperature. The wall temperatures are presented in Figure 5b, indicating that the calcium silicate (CS) material is effective as a thermal barrier at elevated temperatures. Moreover, the expansion joint (EJ) layer exhibited the capability to recover to its original thickness after cooling. These findings are promising for the scalability of the TES system based on the proposed design, which represents a logical next step in the development process. A scaled-up TES bin with a volume of approximately 4.5 m<sup>3</sup> was designed using the same wall structure. The key distinction between this near-scale bin and the small-scale version is that the latter was designed to be tested with stagnant particles, whereas the larger bin allows for particle flow due to the inclusion of a SS316 discharge cone that facilitates particle circulation. The cone is supported by a calcium silicate (CS) base, which separates the cone, the bin's wall, and the contents from the concrete platform on which the bin will be installed. This CS base functions as a thermal barrier, effectively preventing excessive heat from transferring to the concrete platform. The bin is also equipped with a conical lid, which minimizes the ullage volume resulting from the angle of repose of particles. Figure 6 illustrates the design of the near-scale TES bin.

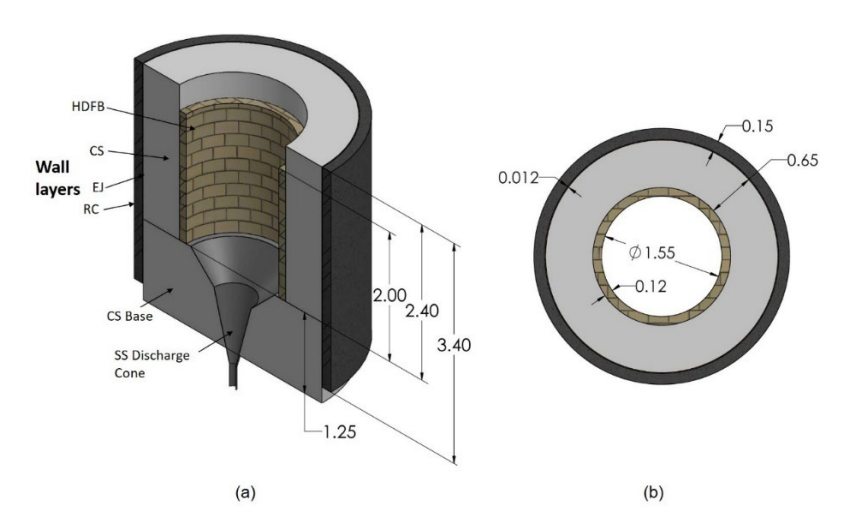


Figure 6. Near-scale TES bin design: (a) sectional 3D view, (b) top view, dimensions in meters

Two near-scale TES bins have been constructed, with the construction stages illustrated in Figure 7. The process can be summarized as follows: first, a reinforced concrete shell is built; next, the discharge cone is installed, followed by the construction of the calcium silicate base underneath. The expansion joint is then added to the concrete shell. Subsequently, the layers of high-density firebrick and calcium silicate for the bin's wall are built simultaneously. Finally, the bin's lid is placed on top.



Figure 7. Construction stages of the near-scale TES bin

# 4. Skip hoist-thermal energy storage integration

A 22-m high concrete tower was built beside the existing KSU's CSP tower. The new tower was built with three platforms to house the PL and the two TES bins. The Two TES bins were constructed on the first and second platforms. The skip-hoist PL was then linked to the two bins through the pre-skip and the upper hopper. The top bin is connected to the PL through the upper hopper and to the bottom bin through the pre-skip. An intermediate hopper has been installed in the pipeline that connects the upper hopper and the top bin, replacing the PHR for the time being. Additionally, an electric heater has been incorporated at the end of this pipeline, just before the top bin. The connection between the top TES bin and bottom TES bin is established using a 4-inch pipe. An additional electric heater has been installed at the end of this pipe, right before the entrance to the bin. A particle loop was finalized by a piping network. Then, the bottom TES bin was first charged with white sand, and a cold run was initiated by circulating the sand within the system. The functionality of the integrated system was demonstrated. Figure 8 shows the integrated system.

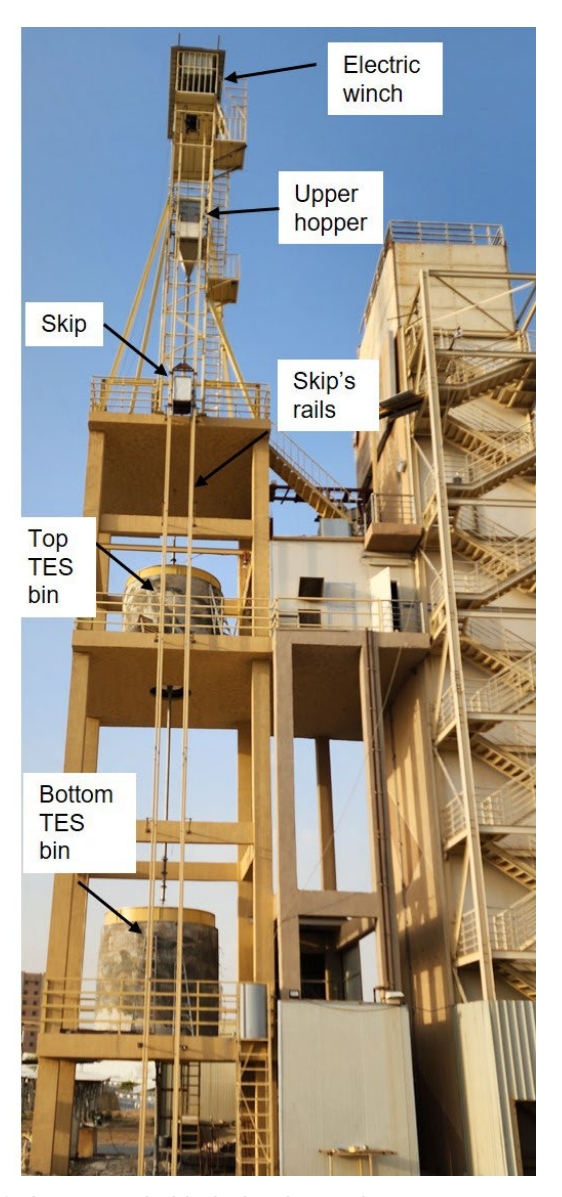


Figure 8. Integrated skip hoist-thermal energy storage system

#### 5. Conclusions

This study successfully demonstrated the proof-of-concept for an integrated skip-hoist particle lift and thermal energy storage (TES) system at ambient temperature, marking a significant advancement in particle-based concentrated solar power (CSP) technology. The skip-hoist particle lift, constructed with stainless steel (SS316) for high-temperature components and optimized with a variable frequency drive (VFD) control system, achieved efficient particle transfer. The multi-layered TES system, incorporating high-density firebrick (HDFB) and calcium silicate layers, exhibited effective thermal insulation and structural integrity, with the expansion joint layer accommodating thermal cycling stresses. Preliminary testing confirmed the operational feasibility of the integrated system, achieving stable particle circulation through a piping network connecting two TES bins on a 22-m concrete tower. These results provide a robust foundation for the proposed 1.3 MWe pre-commercial CSP plant in Waad Al-Shamal, Saudi Arabia, by validating key enabling technologies for scalable, cost-effective particle-based CSP systems. Future work will focus on conducting high-temperature tests at 700 °C and above, optimizing skip speed and TES insulation for commercial-scale deployment, and performing cost analyses to further evaluate economic competitiveness. These advancements will support

the transition of particle-based CSP from proof-of-concept to pre-commercial and commercial applications, contributing to sustainable energy solutions.

# Data availability statement

There is no relevant additional data to this article beyond the presented content.

### **Author contributions**

Conceptualization, N.S.S., S.A., S.J., H.A.-A., E.D.; Methodology, N.S.S., S.A., E.D., S.J.; Resources, H.A.-A.; Investigation, N.S.S., S.A., E.D., R.S.; Formal analysis, N.S.S., S.A.; Visualization, N.S.S.; Validation, H.A.-A., R.S., A.E.-L., Z.A.-S., S.N.D.; Data Curation, Z.A.-S., S.N.D.; Writing - Original Draft, N.S.S.; Writing - Review & Editing, N.S.S., E.D., S.J.; Supervision, H.A.-A., A.E.-L., Z.A.-S.; Funding acquisition, H.A.-A.; Project administration, H.A.-A., S.A., N.S.S..

# **Competing interests**

The authors declare that they have no competing interests.

# Acknowledgement

The authors would like to express their profound gratitude to King Abdullah City for Atomic and Renewable Energy (K.A.CARE) for their financial support in accomplishing this work.

### References

- [1] Saeed, Rageh S., et al. "Characterization of low-cost particulates used as energy storage and heat-transfer medium in concentrated solar power systems." Materials 15.8 (2022): 2946. <a href="https://doi.org/10.3390/ma15082946">https://doi.org/10.3390/ma15082946</a>.
- [2] Alaqel, S., Djajadiwinata, E., Saeed, R. S., Saleh, N. S., Al-Ansary, H., El-Leathy, A., ... & Gandayh, H. (2022). Performance of the world's first integrated gas turbine—solar particle heating and energy storage system. Applied Thermal Engineering, 215, 119049. <a href="https://doi.org/10.1016/j.applthermaleng.2022.119049">https://doi.org/10.1016/j.applthermaleng.2022.119049</a>.
- [3] Sarfraz, Muhammad, et al. "Proposed design and integration of 1.3 MWe pre-commercial demonstration particle heating receiver based concentrating solar power plant." Energy Sustainability. Vol. 84881. American Society of Mechanical Engineers, 2021. https://doi.org/10.1115/ES2021-62529.
- [4] Repole, Kenzo KD, and Sheldon M. Jeter. "Design and analysis of a high temperature particulate hoist for proposed particle heating concentrator solar power systems." Energy Sustainability. Vol. 50220. American Society of Mechanical Engineers, 2016. <a href="https://doi.org/10.1115/ES2016-59619">https://doi.org/10.1115/ES2016-59619</a>.
- [5] El-Leathy, Abdelrahman, et al. "Thermal performance evaluation of lining materials used in thermal energy storage for a falling particle receiver based CSP system." Solar Energy 178 (2019): 268-277. <a href="https://doi.org/10.1016/j.solener.2018.12.047">https://doi.org/10.1016/j.solener.2018.12.047</a>.